Power Spectrum Ranked Independent Component Analysis of a Periodic fMRI Complex Motor Paradigm

Chad H. Moritz,[1]* Baxter P. Rogers,[2] and M. Elizabeth Meyerand[2]

[1]*Department of Radiology, University of Wisconsin, Madison, Wisconsin*
[2]*Department of Medical Physics, University of Wisconsin, Madison, Wisconsin*

Abstract: Independent component analysis (ICA) has been demonstrated to be an effective data-driven method for analyzing fMRI data. However, a method for objective differentiation of task-related components from those that are artifactually non-relevant is needed. We propose a method of constant-cycle (periodic) fMRI task paradigm combined with ranking of spatial ICA components by the magnitude contribution of their temporal aspects to the fundamental task frequency. Power spectrum ranking shares some similarity to correlation with an a priori hemodynamic response, but without a need to presume an exact timing or duration of the fMRI response. When applied to a complex motor task paradigm with auditory cues, multiple task-related activations are successfully identified and separated from artifactual components. These activations include sensorimotor, auditory, and superior parietal areas. Comparisons of task-related component time courses indicate the temporal relationship of fMRI responses in functionally involved regions. Results indicate the sensitivity of ICA to short-duration hemodynamics, and the efficacy of a power spectrum ranking method for identification of task-related components. *Hum. Brain Mapping 18:111–122, 2003.* © 2002 Wiley-Liss, Inc.

Key words: functional magnetic resonance imaging; independent component analysis; motor cortex; human brain mapping; BOLD

INTRODUCTION

Experimental designs for functional MRI (fMRI) paradigms are intended to demonstrate an elicited hemodynamic response from either a stimulus or task [Bandettini et al., 1992; Kwong et al., 1992; Ogawa et al., 1992]. The efficacy of these attempts depends on a multitude of factors, i.e., acquisition hardware, pulse sequence, paradigm design, subject performance, and preserved autoregulation of the hemodynamic response. The resulting fMRI data depend on the choice of post-processing analysis methodology [Bandettini et al., 1993; Friston et al., 1995a,b; Lange and Zeger, 1997; Marchini and Ripley, 2000; Mitra and Pesaran, 1999; Worsley and Friston, 1995; Zarahn et al., 1997] with differing analyses yielding varying sensitivity and specificity to fMRI activations [Lange et al., 1999]. The issue of analysis methodology may be divided into general categories of hypothesis-driven and data-driven techniques [Friston, 1998; McKeown and Sejnowski, 1998]. The former represent methods that

Contract grant sponsor: Whitaker Foundation; Contract grant sponsor: NIH; Contract grant number: RO1 EB00448-01.

*Correspondence to: Chad H. Moritz, Department of Radiology, E1/311 Clinical Sciences Center, 600 Highland Avenue, Madison, WI 53792-3252. E-mail: cmoritz@mail.radiology.wisc.edu

Received for publication 16 July 2001; Accepted 27 September 2002
DOI 10.1002/hbm.10081

combine a priori knowledge of brain function with presumed modeling of hemodynamic response to yield fMRI mapping. While these methods have proven efficacious, it is difficult to hypothesize a model that encompasses all possible responses [Lange et al., 1999; McKeown et al., 1998a,b], especially those that may be unanticipated. The latter category of data-driven analysis attempts to address this concern through methods that do not rely on prior constraints of either hypothetical assumptions or parametric modeling. Because no single fMRI analysis method appears optimized for all situations, it is important to understand both the limits and optimization of applicability for each method [Lange, 1999; Petersson et al., 1999].

Independent component analysis (ICA) is a data-driven method that has been successfully applied to spatial analysis of block-paradigm fMRI datasets [Biswal and Ulmer, 1999; McKeown et al., 1998a,b]. When applied to whole-brain data, ICA has a demonstrated sensitivity to multiple task activations and event-related hemodynamics [Moritz et al., 2000a]. A limitation of purely data-driven analysis is a reliance on presumptions of brain function to retrospectively identify significant fMRI activation patterns from those that are deemed artifactual. A hybrid method of ICA [McKeown, 2000] has been proposed attempting to address the twin issues of 1) separating consistently task-relevant components from those that are non-relevant (and presumably due to artifactual sources such as physiologic noise or motion); and 2) statistical basis for ICA hypothesis testing. This hybrid method has demonstrated utility toward solving both these issues, but it requires the use of an a priori hypothesis to guide the analysis. Thus, the selection of task-related components is limited by the relative timing constraints of a hypothetical response expectation, and the data-driven analysis advantage to delineate unexpected response patterns is compromised.

In an attempt to retain more of the unbiased data-driven sensitivity of ICA, we applied a method of 1) a periodic brief-stimulus fMRI paradigm with constant rates for both stimulus presentation and cued task; 2) spatial ICA analysis of the fMRI data; 3) a Fourier transform of each ICA component time course; and 4) retrospective ranking of the time course for each of the spatial ICA components by their magnitude contribution to the fundamental task frequency. By assuming a periodic paradigm design, the components of variance attributable to the hemodynamic response can be expected to occur at a few discrete frequencies in the spectral domain, these being the fundamental frequency of the activation and its harmonics. Shape, exact timing, and duration of each response need not be modeled [Marchini and Ripley, 2000]. The periodic constancy of the paradigm timing permits each ICA component to be power spectrum rank-ordered at a similar frequency for all task-related activations.

SUBJECTS AND METHODS

Scan Protocol

Seven normal, right-handed volunteers (4 male, 3 female; ages 22–35; mean 27.1 years) were enrolled in the study after first obtaining their informed consent. Additionally, 10 right-handed pre-surgical patients (4 male, 6 female; ages 11–55 years; mean 33 years) performed the task as part of their fMRI mapping protocol. Functional MRI scanning was performed on a 1.5T General Electric Signa LX scanner (GE Medical Systems, Waukesha, WI) equipped with 40 mT/m gradients, using a standard quadrature RF head coil. Foam padding was provided for head support and to help minimize motion. Each subject was fitted with combination earplugs and pneumatic earphones, both to attenuate ambient scanner noise and to provide auditory cues for the complex motor task. Immediately prior to the functional scans, a series of co-registered anatomical images were obtained, including a T1 weighted high-resolution whole-brain volume (3D SPGR; TR/TE 21/7 msec; FA 40 degrees; FOV 24 cm; matrix 256 $\times$ 128; 124 1.2-mm contiguous slice locations). BOLD-weighted fMRI was acquired using a single-shot, gradient-recalled EPI sequence (TR/TE 2,000/40 msec; FA 85 degrees; FOV 24 cm; matrix 64 $\times$ 64; 21 coronal slice locations 6-mm thick/skip 1 mm; receiver bandwidth 125 kHz).

The complex motor task paradigm consisted of fourteen 10-sec task cycles. The auditory cues for this paradigm were produced using Cool Edit 96 software (Syntrillium Software Corporation, Phoenix, AZ), recorded to a CD-ROM, and presented to the subjects inside the scanner via pneumatic stereo hardware. Each task cycle began with the auditory presentation of a set of sinusoidal tones at a fundamental frequency of 600 Hz. The subjects were instructed that during each task cycle, they would first hear a series of auditory tones, followed by an auditory direction of either right or left hand. Their task was to carefully monitor the number, rhythm, and duration of the tonal set, and then to firmly press the index finger to the thumb of the directed hand, one press for each tone in the series, attempting to closely match the duration and temporal pattern of the tone series. The number, rhythm, and duration of these tones varied for each task cycle; each

series of tones lasted approximately 3 sec (timings are approximate, since the tonal pattern varied for each stimulus cycle). Approximately 1 sec after the end of each tonal series, an auditory direction was given of either "right hand" or "left hand." The order of right or left hand directions was pseudo-randomized, and evenly divided, with a total of seven cycles for each hand. After the instruction for hand performance, the remainder of the 10-sec task cycle provided no additional auditory cues. During this interval the subject was to perform the finger-tapping task, and then relax briefly in preparation for the beginning of the next task cycle. Each task cycle followed contiguously, so that presentation of the auditory cues was equally spaced at 10-sec intervals. Combined with the time interval to either listen to each auditory cue or perform each motor task, this resulted in an inter-stimulus-interval (ISI) of approximately 6 sec for either auditory stimulus or motor task. The 14 contiguous task cycles were book-ended by acquisitions of 24 sec of rest before the task began and 16 sec following the end of the last task cycle; no rest intervals were included during the contiguous task performance cycles. A total of 89 EPI scan repetitions were acquired; the 2 sec TR resulted in a scan duration of 2 min, 58 sec.

Prior to the scan, the task was explained and briefly practiced with each subject to ensure their comprehension and ability to perform the task. It was explained that the task was similar to hearing and copying Morse code, that each series of tones would be a different pattern, and the hand instructions would be unpredictable. Each subject was directed to keep their eyes closed during the duration of the scan, to concentrate on performing the task, and to relax their hands when not performing the finger tapping. Subjects were visually monitored by the investigator during the fMRI scan to confirm their correct task performance.

Image Reconstruction and Preprocessing

Raw EPI data were filtered in the spatial frequency domain by use of a low-pass Hamming filter to increase the signal-to-noise ratio [Lowe et al., 1997], and then reconstructed into individual slice-location images. Signal intensities for each image were time-corrected with a 3-point Hanning window shifted to correspond to the temporal offset of the slice acquisition within each 2-sec TR [McKeown et al, 1998b]. A minimum signal threshold was applied to exclude voxels from outside the brain. To minimize pulsation effects from cerebrospinal fluid, all voxels with signal intensity exceeding the average of brain tissue by 2 standard deviations in the first (unsaturated) image of the EPI series were masked from further analysis. A signal-to-noise ratio map (signal to temporal noise) was calculated from the remaining voxels, and those with SNR less than 2 standard deviations below the mean were excluded to minimize physiologic noise contributions from presumed large blood vessels. The AFNI [Cox, 1996] 3D registration algorithm was performed on the datasets to correct for linear motion in six planes; each dataset was coregistered to its own template and structural volume. After discarding the first 4 acquisitions to allow for magnetization steady-state, the resulting matrices from each multislice fMRI dataset had dimensions of 85 timepoints by approximately 10,000 voxels.

Analysis

ICA as formulated by Bell and Sejnowski [1995] was applied to separate the preprocessed images into 85 spatially independent components. Each of these ICA-derived components had an associative spatial mapping, *Z*-score threshold, and corresponding time series. It should be noted that the *Z*-score computed for each individual component merely represent how far the voxel intensities differ from the mean voxel intensity. Moreover, *Z*-score in this context are descriptive measures that correspond to no statistical test. A Fourier transform was applied to each of the component time courses to obtain a frequency power spectrum. These power spectra were ranked in descending order by their magnitude contributions at the fundamental frequency of the task cycles (0.1 Hz). Spatial mappings for each component were thresholded at $Z > 2.5$ and viewed with the AFNI display program overlaid on the coregistered MRI structural volumes. Spatial and temporal patterns of all the resulting components were then inspected for confirmation of patterns relevant to the task performance. ICA components that demonstrated 1) power spectrum characteristics that matched the task frequency; 2) signal changes temporally correlated to the task; and 3) spatial mappings to relevant areas of activation, were tabulated for their spatial mapping(s) and rank order for each subject.

The ICA components that were identified as being task-related were then further analyzed to assess a measure of significance in the power spectra. First, the independent component time series were linearly detrended to remove low frequency artifacts. Periodograms of the de-trended component time series were estimated and smoothed with a bandwidth of 0.00424 Hz in the R statistical package (available online at http://www.r-project.org). The significance of the

0.1-Hz peaks was tested under the null hypothesis of white noise, and a threshold value of $P < 0.05$ was considered significant.

For comparison purposes to a standard statistical test, the datasets from the seven normal subjects were submitted to a regression analysis with sine and cosine waves at the fundamental 0.1-Hz task frequency. Like ICA, this analysis design does not make assumptions of either phase or shape of the hemodynamic response. The program SPM99 [Friston et al., 1995a] was used to perform an F-test on the two regressors simultaneously, which was thresholded at $P < 0.001$ (uncorrected). The resulting statistical maps were inspected and compared to spatial ICA maps previously identified as being task-relevant.

RESULTS

All of the subjects were visually observed to have performed the task accurately, and head motion was minimal for most subjects. For each of these 17 subjects, singular ICA components were identified that were specific to 1) right hand motor activation areas of left sensorimotor cortex [Brodman's areas (BA) 1, 3, and 4], left supplementary motor area (BA 6), and right superior cerebellum; 2) left hand motor activation areas of right sensorimotor cortex (BA 1, 3, and 4), right supplementary motor area (BA 6), and left superior cerebellum (Fig. 1A,B). Time courses for these motor activation components indicated their correspondence to the right and left hand task activation cycles (Fig. 2A, row 1). For 14 of the 17 subjects, ICA produced a separate component that was specific to bilateral primary and secondary auditory cortex (BA 41 and 42) (Fig. 1C); time courses were synchronous with the auditory cues (Fig. 2A, row 2). For 8 of the 17 subjects, a component was identified that mapped to bilateral areas of the superior parietal gyrus (BA 7) (Fig. 1D). The time course of this component indicated a slight signal increase that frequently occurred between the cued auditory response and the initiation of the finger task cycles (Fig. 2A, row 3). In six of these eight subjects, the same bilateral superior parietal component also mapped to an area of either right, left, or bilateral middle frontal gyrus. In 5 of the 17 subjects, a separate component was identified that mapped to areas of bilateral putamen (Fig. 1E). The time courses of these putamen-specific components were inconsistently synchronized with the task timing (Fig. 2A, row 4). The time courses for all these spatial ICA components demonstrated a hemodynamic delay of approximately 6 sec to signal peak, as distinguished by the 2-sec TR.

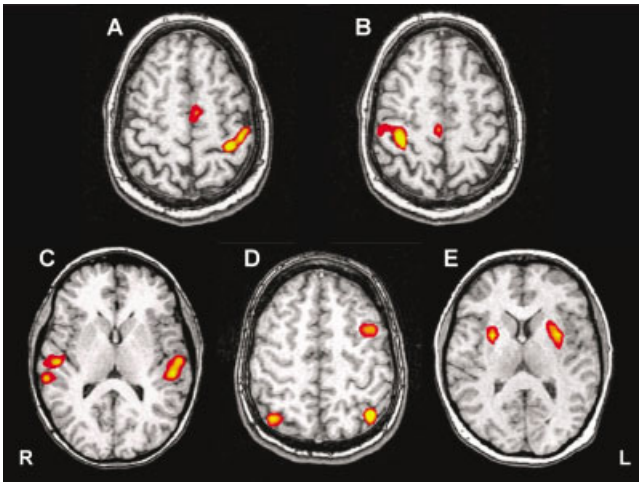

Figure 1.
Spectral ranked ICA-identified task-related spatial maps. Shown are representative singular ICA task-relevant component maps for: (**A**) Primary sensorimotor and supplementary motor area activations for left hand finger task; (**B**) Primary sensorimotor and supplementary motor area activations for right hand finger task; (**C**) Bilateral auditory activations for auditory task cues; (**D**) Bilateral superior parietal and left middle frontal gyrus regions; (**E**) Bilateral anterior putamen. Note: all figures are radiologic convention. Color scales for *Z*-score values are red = 2.5–3.5; orange = 3.5–4.5; yellow > 4.5.

Power spectrum ordering of the Fourier transform of each ICA component time course by its contribution at the fundamental 0.1-Hz task frequency ranked each of the identified task-related components within the first ten. None of the task-related components was ranked higher than 10th (out of 85), and often the first few ranked components were task-related (Table I). The average power spectrum rank for the identified task-related components was 2.36 for bilateral auditory; 2.71 for right hand motor; 3.41 for left hand motor; 4.6 for bilateral putamen; and 6.0 for superior parietal. Fourier transform plots of each component time course revealed the spectral peak at 0.1 Hz for

Figure 2.
Time courses and Fourier transform plots of spectral ranked ICA-identified task-related components. Shown are representative signal vs. time time course graphs (**A**) and their respective Fourier transform plots (**B**) for combined right and left hand motor activations (row one); bilateral auditory (row 2); superior parietal (row 3); and bilateral putamen (row 4). Vertical line spacings in the time course graphs indicate initiation, without allowance for hemodynamic delay, of each motor paradigm task cycle. R = right hand; L = left hand; T = auditory cue. These plots correspond to the same ICA component spatial maps shown in Figure 1.

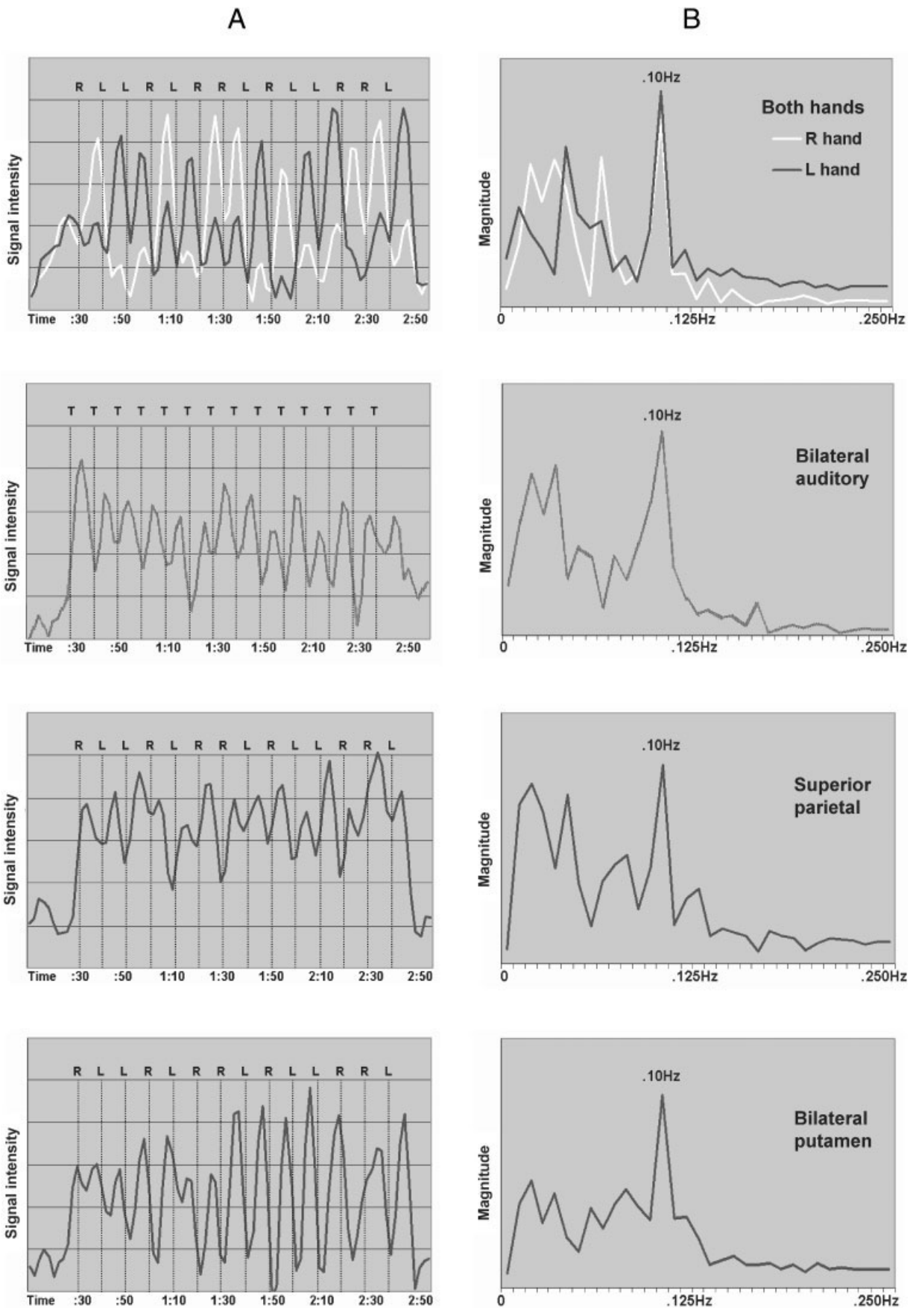
A
B
R L L R L R R L R L L R R L
Signal intensity
Time :30 :50 1:10 1:30 1:50 2:10 2:30 2:50
.10Hz
Magnitude
0 .125Hz .250Hz
Both hands
R hand
L hand
T T T T T T T T T T T T T T
Bilateral auditory
Superior parietal
Bilateral putamen

Figure 2.

TABLE I. Power spectrum ICA ranking results of 5 identified task-relevant components*

Subject no.	Identified task-related components				
	Right-hand motor	Left-hand motor	Bilateral auditory	Superior parietal	Bilateral putamen
1	4	10	1	9	—
2	2	7	1	6	—
3	3	2	1	—	—
4	3	1	—	4	2
5	2	5	1	—	3
6	1	2	4	7	—
7	3	1	2	10	—
8	3	5	1	7	—
9	1	2	4	—	6
10	3	2	1	—	4
11	1	6	7	—	—
12	10	4	1	—	—
13	2	1	4	3	—
14	2	1	4	—	7
15	1	2	—	—	—
16	2	1	—	—	—
17	3	6	1	2	—

* Ranking numbers are in descending order out of 85 total ICA components, with lower numbers indicating a higher ranking. Subjects 1–7 were the normal controls; Subjects 8–17 were the presurgical fMRI mapping patients. Dashes indicate that this component was not found.

each of the task-related independent components (Fig. 2B). When these time series were linearly de-trended and their periodograms smoothed, all task-related components surpassed a $P < 0.05$ significance test under the null hypothesis of white noise. Notably, the 0.1-Hz power spectrum ranking for the right and left hand sensorimotor components was effective even though the task timing for each individual hand did not have the same frequency of occurrence as the overall task timing. Examination of the spatial ICA-derived sensorimotor component time courses revealed a shared ipsi- and contralateral response to each of the 14 task cycles (Fig. 2A, row 1). As expected, the contralateral sensorimotor response was greater than the ipsilateral response. The lesser ipsilateral sensorimotor responses were sufficient to contribute toward these components' magnitude frequency contribution at the overall task rate of 0.1 Hz.

Comparison results of the conventional regression analysis using the sine/cosine waves at 0.1 Hz on the seven normal subjects yielded a consistent pattern. All seven datasets demonstrated fMRI mapping to bilateral auditory regions (BA 41 and 42), and five of the seven also showed supplementary motor area response (BA 6), at the F-test threshold of $P < 0.001$ (uncorrected). However, only one dataset showed a suprathreshold fMRI mapping to a region of primary sensorimotor cortex (BA 1, 3, and 4) with this analysis. With frequency-ranked ICA, bilateral auditory response was seen in six of these seven, and bilateral primary and supplementary motor area responses were identified in all seven of these datasets (Table I, Subjects 1–7). fMRI mappings to areas of superior parietal and putamen, which were seen inconsistently with ICA, were not identified with this method of simple sine/cosine regression.

The spatial ICA components that were not identified as being consistently task-related were presumed to represent signal sources such as physiologic noise or motion artifact. The combined criteria of 1) power spectrum magnitude at the 0.1-Hz task frequency; 2) synchrony with the timing of the periodic task cycles; and 3) spatial mappings corresponding to likely patterns of fMRI task response, were applied to the inspection of these non task-related components. Spatial mappings that were discounted included those with no recognizable functional pattern, such as signal appearing strictly in one coronal slice location, or signal appearing at the periphery of the head and likely arising from motion artifact. All of the non-consistently task-related components failed to demonstrate a match to these three criteria, and were discounted from tabulation. A representative example of how signal contributions from a pulsatile venous flow ICA component are lower ranked with the power spectrum ranking method is shown in Figures 3A and 4A,B. The time course from the artifactual pulsatile component, which mapped to the region of straight sinus, demonstrated a signal pattern that often matched the task timing cycles. Power spectrum ranking indicated a frequency peak at .09 Hz for this pulsatile component

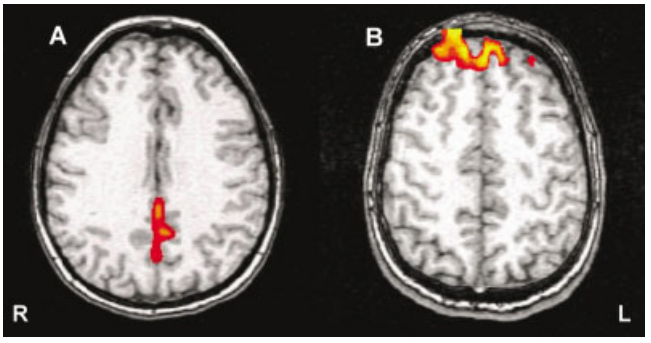

Figure 3.
Spatial mappings of spectral-ranked ICA-derived artifactual components. **A:** Pulsatile venous flow artifact in straight sinus. **B:** Head motion artifact in frontal pole.

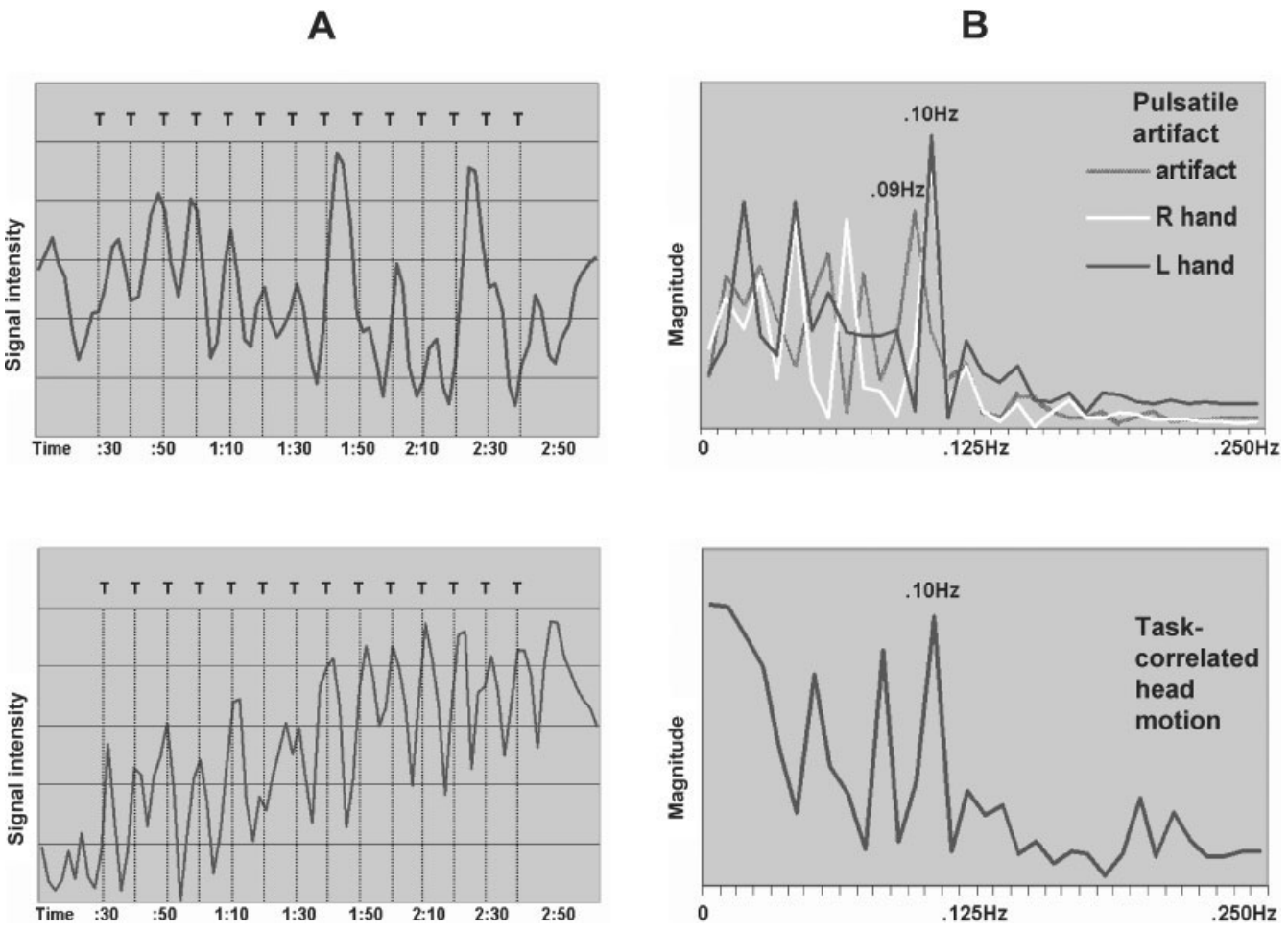

Figure 4.

Time courses and Fourier transform plots of spectral-ranked ICA-derived artifactual components. Time-course plots in column **A** correspond to Fourier plots in column **B**. Shown in row 1 is the pulsatile flow artifact that mapped to straight sinus, the same component as mapped in Figure 3A. The Fourier graph of this pulsatile artifact component has been overlaid with the task-relevant right and left hand finger motor components from the same subject for comparison of their spectral peaks. Row 2 shows the task-correlated head motion artifactual component that is mapped in Figure 3B.

that was close, but did not match the task frequency. For this subject, power spectrum ranking listed the left- and right-hand motor components as 1st and 2nd, respectively, while the pulsatile artifact component was ranked 15th. Similarly, Figures 3B and 4A,B show an example of a frontal head motion artifact. The time course of this spatial ICA-defined motion artifact was closely correlated with the task timing, and had a 0.1-Hz power spectrum ranking of 4th for this subject. Auditory, right- and left-hand components were ranked 1st, 2nd, and 5th for this subject. The artifactual nature of this spatial ICA component was readily identified by its specific spatial mapping to region of prefrontal pole, an area of the brain that is sensitive to a common "nodding" motion artifact along the pitch axis. Otherwise, this task-related motion artifact was highly ranked by power spectrum ordering, and presumably would have also been observed with a linear regression analysis.

When the time courses associated with each of the task-related spatial ICA components were overlaid, it was possible to deduce a direct comparison of the temporal responses in each activated region. This comparison included the temporal relationship of identified fMRI response across regions, but due to unique scaling factors in the ICA algorithm caused by limitations on the uniqueness of solutions to the blind source separation problem [Comon, 1994], it was not possible to directly compare the magnitude of responses across different ICA components. Figure 2A

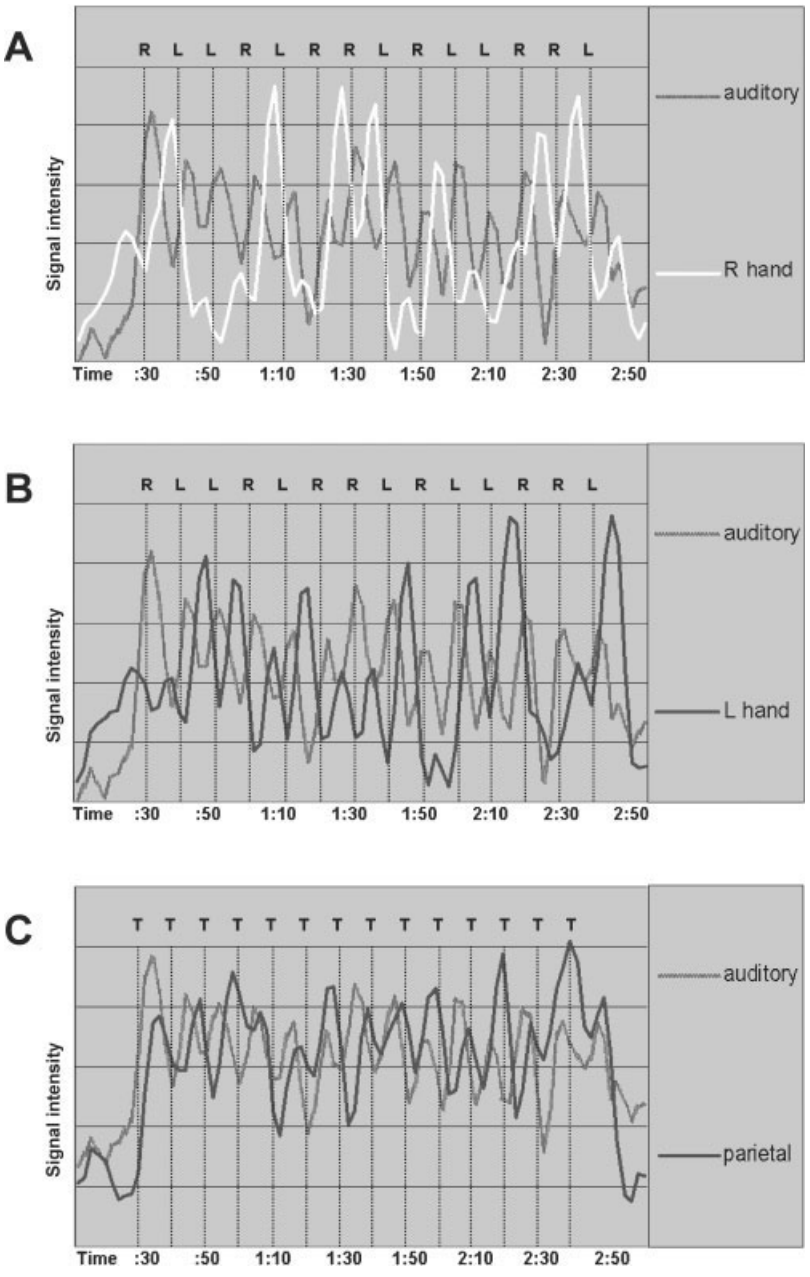

Figure 5.
Time course overlays of ICA task-related components. Signal vs. time plots comparing ICA component temporal hemodynamic responses for (**A**) bilateral auditory and right hand motor components; (**B**) bilateral auditory and left hand motor components; (**C**) bilateral auditory and superior parietal components. Figure 2A features a similar overlay comparing right and left hand motor components. All comparison plot overlays are from the same subject. Vertical line spacings in the time course plots indicate initiation, without allowance for hemodynamic delay, of each motor paradigm task cycle. R = right hand; L = left hand; T = auditory cue.

(row 1) and Figure 5 show examples of comparative temporal responses from identified ICA components from right and left sensorimotor, bilateral auditory, and superior parietal gyri. The temporal relationship of these separate components demonstrated an auditory response early in each task cycle, followed by a brief response in superior parietal regions and the sensorimotor response for the appropriate hand activation. These comparative time courses were derived from each of the associated spatial ICA components, and did not involve averaging or grouping across task cycles. The transient ICA-delineated hemodynamic responses to each of the 14 individual task cycle events can be directly compared. The relative magnitude of response across task cycles can be observed when the comparison is limited to a single ICA component timecourse.

DISCUSSION

This exploratory study demonstrates the utility of a power spectrum domain ranking of spatial ICA-derived fMRI components applied to a periodic motor paradigm of short duration task cycles and interstimu-

lus delays. Multiple task-related fMRI activation maps were identified and highly ranked among the 85 total components. The power spectrum ordering of the ICA components generally ranked non task-related components lower than those that were task-related. This ranking method, combined with retrospective inspection of component time courses and spatial maps, effectively separated artifact and noise from fMRI activation.

The task-related components accurately mapped to expected areas of sensorimotor and auditory activation, as well as bilateral superior parietal lobes, middle frontal gyrus, and anterior putamen. The sensorimotor, auditory, and putamen activation maps were similar to previous whole-brain ICA results from a block fMRI motor paradigm [Moritz et al., 2000a]. The task paradigm and ICA were particularly effective in demonstrating supplementary motor area mapping, with the robust supplementary motor area BOLD response presumably due to the complexity and varying iterations of the motor task. The spatially independent components from eight of the subjects that mapped to superior parietal and frontal lobes are similar to regions that have been implicated in previous fMRI studies for activity related to visual-spatial orientation of motor function [Villar et al., 1999; Wexlar et al., 1997]. The varying complexity of this motor paradigm, and its randomization of right and left functions, would be expected to involve similar cognitive areas. It is not known why these activation patterns were not detected more frequently in this study group. Further research would be needed to determine if these activation patterns were not observed more frequently due to factors of BOLD response, ICA sensitivity, paradigm design, and/or subject performance. Similarly, the putamen-specific activation was only seen in 5 of 17 subjects. This detection ratio is similar to spatial ICA results from a block motor paradigm [Moritz et al., 2000a], but a lower detection ratio than with a *t*-test using a brief-stimulus response function timed to task initiation in a block motor paradigm [Moritz et al., 2000b]. The paradigm design, with slight delay between cued auditory stimulus and performance of hand task, would be expected to involve cognitive networks of working memory. For unknown reasons, spatial ICA did not consistently define a working memory cognitive response pattern. However, 6 of the 8 subjects that had an identified task-related component mapping to superior parietal areas showed a mapping in frontal regions within the same spatial component. These regions of dorsolateral prefrontal cortex might putatively be involved with a working memory cognitive response, but the inconsistency of identified response within these structures does not adequately define a working memory activation.

Thresholding effects of ICA spatial overlays differ from thresholding of regression analysis maps. Each ICA component map represents a distribution of voxels that have a varying contribution to the spatial independence criteria for that unique component. Varying the threshold will demonstrate the contribution of suprathreshold voxels to that individual component, but this represents only a fraction of the total image data. The $Z > 2.5$ threshold applied in this study was chosen as a reasonable representation of the spatial configuration for each component. A higher threshold might yield an increased spatial specificity to the maps, but a lower threshold would not be expected to yield different activation patterns that are not already apparent. Thus, the response patterns for activations in auditory, putamen, and parietal regions that were not seen in the ICA of all subjects would not be expected at lower threshold display levels.

It is notable that the combination of a complex motor paradigm and spatial ICA were successfully applied across a broad range of subjects, including a clinical patient population with an age range from 11 to 55 years. When motion correction was applied to these data sets, some of the patients demonstrated head motion greater than 1 mm, occasionally correlated with the task timing. In cases of task-correlated head motion, the power spectrum ordering of the spatial components assigned a high ranking to some of these artifactual motion-related components. However, visual inspection of the motion-related spatial maps demonstrated their artifactual character. In this study, the spatial ICA algorithm segregated motion artifact into separate independent components from the multiple task-relevant activations in sensorimotor and auditory regions. A more specific assessment of ICA sensitivity to motion artifact may warrant further research.

The power spectrum ranking of spatial ICA has demonstrated sensitivity to hemodynamic response patterns that are consistently task-related, even when the relative timing and duration of these responses are variable and of short duration. The ICA method effectively delineated task responses of short duration (~4 sec) and short ISI (~6 sec) employed in this task paradigm. The combination of brief stimuli and task cycles, with brief ISIs, resulted in a relatively dense fMRI paradigm that lasted less than 3 min. Previous reports [Biswal and Ulmer, 1999; Calhoun et al., 2001; McKeown et al., 1998a,b; Moritz et al, 2000a] have not applied ICA to fMRI paradigms with short-epoch, short-ISI design. Analysis methods that rely on a lin-

ear modeling of the hemodynamic response would predictably yield a low efficiency of detection and estimation when applied to a single trial, periodic paradigm of short duration and fixed ISI [Dale, 1999; Liu et al., 2000a]. Event-related regression methods, such as SPM, assume a fixed hemodynamic response for each event, whereas ICA is sensitive to event variability. As demonstrated in this study, the data-driven nature of spatial ICA, which does not rely on a linear or non-linear BOLD model, is sufficiently sensitive to short-duration, short-ISI hemodynamic response paradigm designs. Temporal ICA, which was not applied in this study, can yield different sensitivities to paradigm designs [Calhoun et al., 2001]. However, temporal ICA when applied to whole-brain fMRI data is limited by computational demands [Friston, 1998]. Further investigation with varying task durations and ISIs might yield more information about ICA sensitivity to BOLD hemodynamics.

Task relevance is an important consideration for the interpretation of data-driven analysis. As stated by McKeown [2000], purely data-driven techniques lack a direct means for hypothesis testing. The significance testing of the independent component spectral peaks at the task frequency of 0.1 Hz does not in itself confirm a task-relevance. The power spectrum ranking was applied in this study not as a measure of significance, but rather as a hierarchical ordering of the independent components. Thus, for confirmation purposes, we evaluated the component task-relevance by inspection for spatial mappings to regions of known activation and time course correlation. The power spectrum ranking similarly applies an a priori assumption of task frequency, but precludes a necessity for precise modeling of response shape, duration, or relative timing. An example of when the power spectrum information might be efficacious could occur in a case where a consistent task-related response is temporally delayed, and in an unexpected cortical region. The power spectrum ordering shares some similarity to simple correlation, but without phase sensitivity. The lack of phase sensitivity, when applied to this paradigm, allowed for identification of multiple task responses that occurred within different temporal phases of each task cycle. At least three separate reference function correlations would need to be performed to obtain similar identification of the multiple task-correlated components that were selectively ranked at a single frequency. A caveat of designing periodic paradigms for spectrum rank ordering might be the avoidance of physiologic signals for cardiac and respiratory cycles. These could occur in the range of 0.1–1.2 Hz for respiratory, and 0.6–1.2 Hz for cardiac [Cordes et al, 2001], unless aliased by the TR sampling rate.

Other methods have been proposed and applied toward hierarchical ranking of fMRI ICA components. As discussed, McKeown et al. [1998a, 2000] have effectively used correlation with a task-related reference function to identify relevant components. However, this a priori correlation compromises the purely data-driven possibilities for discovering unexpected fMRI responses. Other, more data-derived ranking method attempts have been based on Z-score [Cordes et al., 1999], entropy [Liu et al., 2000b], kurtosis, or clustering [Esposito et al., 2001]. These methods alone have not been successful in their attempts toward a fully automatic classification, since fMRI response distributions do not always match criteria for greatest variance, least spatial structure, "non-Gaussianity," or spatial extent.

A limitation of the power spectrum ranking applied in this study is that it is optimized for use with a periodic fMRI paradigm, with the independent components ranked according to their contribution at a constant task frequency. This type of analysis would be less efficacious if the subject's response is erratic in terms of the brain region being activated or the temporal pattern of activation (failure to perform the task consistently). The right and left hand task cycles in this study's fMRI paradigm did not have the same timing rate, but some sensorimotor activation was shared both ipsi- and contralaterally. Thus, the 0.1-Hz power spectrum ranking at the fundamental frequency of the overall task was effective for these sensorimotor components. Cognitive tests that employ randomization of events to minimize confounding performance effects such as habituation or anticipation might not be applicable to this method. In such cases, a correlation of spectral densities between the randomized paradigm cycles and the spatial ICA-derived time courses might provide a means of identifying consistently task-related BOLD responses. A correlation of spectral densities is beyond the scope of this study.

Statistical inferences such as those drawn from parametric testing of fMRI data [Friston et al., 1995a] do not have an identical corollary with the non-parametric ICA. The methods employed by statistical parametric mapping for derivation of confidence values for hypothesis testing (i.e., P values) are not available for ICA results due to the absence of a null hypothesis [Friston, 1998]. The spatial ICA fMRI maps in this study do not have an associated P value that indicates a confidence level asserting a hypothetical activation. Application of a $P < 0.05$ threshold to the derived Fourier transforms of the component time courses for

the task frequency peak at 0.1 Hz indicated that all task-related components surpassed this threshold. However, the power spectrum ranking method did not involve a level of confidence testing, and merely relied on a value contribution at the task frequency. The trade-off with non-parametric analysis is a complementary data decomposition that is sensitive to complex and unanticipated hemodynamic responses [Friston, 1998; McKeown and Sejnowski, 1998]. The dynamic nature of the human brain response requires a matching level of statistical complexity [Lange, 1999]. In this study, the ICA-derived components were selectively tested for task relevance by power spectrum rank-order, and confirmed with time course response timing and spatial mapping. A method for comprehensively deriving a corresponding confidence statistic from the combination of these observations has not yet been defined.

Comparison to the conventional statistical analysis with an effects-of-interest regression using the sine/cosine waves at the fundamental task frequency of 0.1 Hz indicated that this SPM method is sensitive to the auditory and supplementary motor area responses. The regression analysis was less sensitive than ICA to the primary sensorimotor responses for this task paradigm. This indication is reasonable, since the auditory cues for the task paradigm were periodic while the individual hand task performance cycles were not. Presumably, the overlap in supplementary motor area response from each hand task cycle provided sufficient periodicity for this region to map in five of the seven normal subjects with the sine/cosine regression. This comparison to a simple hypothesis testing at the fundamental task frequency demonstrates that the combination of spatial ICA with frequency ranking has greater sensitivity to multiple task-related responses from this complex motor paradigm. As stated previously, multiple regressors would need to be applied to obtain a set of fMRI maps similar to those derived with ICA. The voxel-wise task-related frequency content alone does not provide sufficient specificity to derive the spatial localizations that were delineated by ICA of this paradigm.

CONCLUSION

The aim of this study was to apply a power spectrum ranked independent component analysis method to a periodic fMRI complex motor paradigm. The main conclusions are: 1) spatial ICA effectively delineated multiple task-related components from the raw fMRI data across all 17 subjects. 2) These task-related components were separated from artifact and physiologic noise, even though the stimuli and motor responses were of short duration with short interstimulus intervals. 3) Power spectrum ranking of the spatial ICA components at the .1-Hz task frequency generally gave a higher rank order to task-related components than to those from artifactual or other noise sources. This power spectrum ranking ICA method does not rely on modeling of a presumed hemodynamic response or phase information, and thus may have utility toward the discovery of fMRI responses with unexpected timing or duration.

ACKNOWLEDGMENTS

This work was funded in part by grants from the Whitaker Foundation and the National Institutes of Health (R01 EB00448-01 to M.E.M.).

REFERENCES

Bandettini PA, Cox RW. 2000. Event-related fMRI contrast when using constant interstimulus interval: theory and experiment. Magn Reson Med 43:540–548.

Bandettini PA, Wong EC, Hinks RS, Tikofsky RS, Hyde JS. 1992. Time course of human brain function during task activation. Magn Reson Med 25:390–397.

Bandettini PA, Jesmanowicz AJ, Wong EC, Hyde JS. 1993. Processing strategies for time-course data sets in functional MRI of the human brain. Magn Reson Med 30:161–173.

Bell AJ, Sejnowski TJ. 1995. An information-maximization approach to blind separation and blind deconvolution. Neural Comput 7:1129–1159.

Biswal BB, Ulmer JL. 1999. Blind source separation of multiple signal sources of fMRI data sets using independent component analysis. J Comp Assist Tomogr 23:265–271.

Calhoun VD, Adali T, Pearlson GD, Pekar JJ. 2001. Spatial and temporal independent component analysis of functional MRI data containing a pair of task-related waveforms. Hum Brain Mapp 13:43–53.

Comon P. 1994. Independent component analysis: A new concept? Signal Process 36:11–20.

Cordes D, Carew J, Eghbalnia H, Meyerand E, Quigley M, Arfanakis K, Assadi A, Turski P, Haughton V. 1999. Resting-state functional connectivity study using independent component analysis. Proceedings 7th International Conference ISMRM, Philadelphia. p 1706.

Cordes D, Haughton VM, Arfanakis K, Carew JD, Turski PA, Moritz CH, Quigley MA, Meyerand ME. 2001. Frequencies contributing to functional connectivity in the cerebral cortex in "resting-state" data. Am J Neuroradiol 22:1326–1333.

Cox RW. 1996. AFNI: Software for analysis and visualization of functional magnetic resonance neuroimages. Comp Biomed Res 29:162–173.

Dale AM. 1999. Optimal experimental design for event-related fMRI. Hum Brain Mapp 8:109–114.

Esposito F, Formisano E, Cirillo S, Elefante R, Tedeschi G, Goebel R, Di Salle F. 2001. Criteria for the rank ordering of fMRI independent components. Proceedings 7th Annual Meeting OHBM, Brighton, UK. p 114.

Friston KJ. 1998. Modes or models: a critique on independent component analysis for fMRI. Trends Cognit Sci 2:373–375.

Friston KJ, Holmes AP, Worsley KJ, Poline CD, Frith, Frackowiak RSJ. 1995a. Statistical parametric maps in functional imaging: a general linear approach. Hum Brain Mapp 2:189–210.

Friston KJ, Holmes AP, Poline CD, Grasby PJ, Williams SCR, Frackowiak RSJ, Turner R . 1995b. Analysis of fMRI time-series revisited. Neuroimage 2:45–53.

Kwong KK, Belliveau JW, Chesler DA, Goldberg IE, Weisskoff RM, Poncelet BP, Kennedy DN, Hoppel BE, Cohen MS, Turner R, Cheng H-M, Brady TJ, Rosen BR. 1992. Dynamic magnetic resonance imaging of human brain activity during primary sensory stimulation. Proc Natl Acad Sci U S A 89:5675–5679.

Lange N. 1999. Statistical thinking in functional and structural magnetic resonance neuroimaging. Stat Med 18:2401–2407.

Lange N, Zeger SL. 1997. Non-linear fourier time series analysis for human brain mapping by functional magnetic resonance imaging. Appl Stat 46:1–29.

Lange N, Strother SC, Anderson JR, Nielsen FA, Holmes AP, Kolenda T, Savoy R, Hansen LK. 1999. Plurality and resemblance in fMRI data analysis. Neuroimage 10:282–303.

Liu TT, Miller KL, Wong EC, Frank LR, Buxton RB. 2000a. Using image entropy to select meaningful spatial maps in independent component analysis. Proc 8th International Conference ISMRM, Denver, CO. p 847.

Liu TT, Frank LR, Wong EC, Buxton RB. 2000b. Detection power, estimation efficiency, and predictability in event-related fMRI. Neuroimage 13:759–773.

Lowe MJ, Sorenson JA. 1997. Spatially filtering functional magnetic resonance imaging data. Magn Reson Med 37:723–729.

Marchini JL, Ripley BD. 2000. A new statistical approach to detecting significant activation in functional MRI. Neuroimage 12:366–380.

McKeown MJ. 2000. Detection of consistently task-related activation in fMRI data with hybrid independent component analysis. Neuroimage 11:24–35.

McKeown MJ, Sejnowski TJ. 1998. Independent component analysis of fMRI data: examining the assumptions. Hum Brain Mapp 6:368–372.

McKeown MJ, Jung T-P, Makeig S, Brown GC, Kindermann SS, Lee T-W, Sejnowski TJ. 1998a. Spatially independent activity patterns in functional magnetic resonance imaging data during the Stroop color-naming task. Proc Natl Acad Sci U S A 95:803–810.

McKeown MJ, Makeig S, Brown GC, Jung T-P, Kindermann SS, Bell AJ, Sejnowski TJ. 1998b. Analysis of fMRI data by blind separation into independent spatial components. Hum Brain Mapp 6:160–188.

Mitra PP, Pesaran B. 1999. Analysis of dynamic brain imaging data. Biophys J 76:691–708.

Moritz CH, Haughton VM, Cordes D, Quigley MA, Meyerand ME. 2000a. Whole-brain functional MR imaging activation from a finger-tapping task examined with independent component analysis. Am J Neuroradiol 21:1629–1635.

Moritz CH, Meyerand ME, Cordes D, Haughton VM. 2000b. Functional MR imaging activation after finger tapping has a shorter duration in the basal ganglia than in the sensorimotor cortex. Am J Neuroradiol 21:1228–1234.

Ogawa S, Tank DW, Menon R, Ellermann JM, Kim SG, Merkle H, Ugurbil K. 1992. Intrinsic signal changes accompanying sensory stimulation: functional brain mapping with magnetic resonance imaging. Proc Natl Acad Sci U S A 89:5951–5955.

Petersson KM, Nichols TE, Poline JB, Holmes AP. 1999. Statistical limitations in functional neuroimaging. Non-inferential methods and statistical models. Phil Trans R Soc Lond B Biol Sci 354: 1239–1260.

Villar G, Lobel E, Galati G, Berthoz A, Pizzamiglio L, Le Bihan D. 1999. A fronto-parietal system for computing egocentric spatial frame of reference in humans. Exp Brain Res 124:281–286.

Wexlar BE, Fulbright RK, Lacadie CM, Skudlarski P, Kelz MB, Constable RT, Gore JC. 1997. An fMRI study of the human cortical motor system response to increasing functional demands. Magn Reson Imag 15:385–396.

Worsley KJ, Friston KJ. 1995. Analysis of fMRI time series revisited: again. Neuroimage 2:173–181.

Zarahn E, Aguirre GK, D'Esposito MD. 1997. Empirical analysis of BOLD fMRI statistics. Neuroimage 5:179–197.